Synthesis of Hexaruthenium Bis(arene) Clusters. Molecular and Crystal Structure of $[Ru_6C(CO)_{11}(\eta^6\text{-}1,3,5\text{-}C_6H_3Me_3)(\eta^6\text{-}C_6H_6)]$ and $[Ru_6C(CO)_{11}(\eta^6\text{-}1,3,5\text{-}C_6H_3Me_3)_2]$

Dario Braga,* Fabrizia Grepioni, and Sandra Righi

Dipartimento di Chimica "G. Ciamician", Università di Bologna, Via Selmi 2, 40126 Bologna, Italy

Paul J. Dyson and Brian F. G. Johnson*

Department of Chemistry, University of Edinburgh, West Mains Road, Edinburgh EH9 3JJ, U.K.

Philip J. Bailey and Jack Lewis*

University Chemical Laboratory, Lensfield Road, Cambridge CB2 1EW, U.K.

Received May 6, 1992

Treatment of $[Ru_6C(CO)_{14}(\eta^6\text{-}1,3,5\text{-}C_6H_3Me_3)]$ with 2 equiv of Me_3NO in CH_2Cl_2 in the presence of 1,3-cyclohexadiene yields the mixed arene–diene derivative $[Ru_6C(CO)_{12}(\eta^6\text{-}1,3,5\text{-}C_6H_3Me_3)(\eta^4\text{-}C_6H_8)]$ (**2**). Further reaction of **2** with Me_3NO/CH_2Cl_2 produces $[Ru_6C(CO)_{11}(\eta^6\text{-}1,3,5\text{-}C_6H_3Me_3)(\mu_3\text{:}\eta^2\text{:}\eta^2\text{:}\eta^2\text{-}C_6H_6)]$ (**3**), which, on standing, converts to a second isomer $[Ru_6C(CO)_{11}(\eta^6\text{-}1,3,5\text{-}C_6H_3Me_3)(\eta^6\text{-}C_6H_6)]$ (**4**). In a similar sequence of reactions employing $1,3,5\text{-}C_6H_5Me_3$, the complexes $[Ru_6C(CO)_{12}(\eta^6\text{-}1,3,5\text{-}C_6H_3Me_3)(\eta^4\text{-}1,3,5\text{-}C_6H_5Me_3)]$ (**5**) and $Ru_6C(CO)_{11}(\eta^6\text{-}1,3,5\text{-}C_6H_3Me_3)_2]$ (**6**) have been obtained. The molecular structures of **4** and **6** in the solid state have been characterized by single-crystal X-ray diffraction. Complex **4** is orthorhombic, space group *Pbca*, with a = 15.996 (5) Å, b = 15.997 (5), c = 23.81 (1) Å, V = 6093.7 Å^3, Z = 8, D_c = 2.45 g·cm^{-3}, $F(000)$ = 4256, final R = 0.035, and R_w = 0.033 for 1728 out of 5896 independent reflections [$I_0 > 2\sigma(I_0)$]; **6** is monoclinic, space group $P2_1/c$, with a = 10.084 (1) Å, b = 16.984 (3) Å, c = 19.425 (5) Å, β = 88.94 (1)°, V = 3326.4 Å^3, Z = 4, D_c = 2.33 g·cm^{-3}, $F(000)$ = 2224, final R = 0.032, and R_w = 0.035 for 4437 out of 6321 independent reflections [$I_0 > 2\sigma(I_0)$]. It has been shown that in **4** the two arenes are terminally bound on adjacent ruthenium atoms, while in **6** the Ru_6C-cluster unit is sandwiched between the two mesitylene ligands. The molecular organization in crystalline **4** and **6** has been investigated by empirical packing potential energy calculations showing that, in both cases, the arene ligands establish graphitic-like intermolecular interactions in the lattice.

Introduction

The synthesis of the first arene cluster compounds $[Ru_6C(CO)_{14}(\eta^6\text{-arene})]$ (arene = $C_6H_3Me_3$, $C_6H_4Me_2$, C_6H_5Me) was reported several years ago[1a,b] and the η^6-coordination mode established by an X-ray diffraction study of the mesitylene derivative.[1c] Later we demonstrated[2] that, on treatment with NaOH/MeOH, these derivatives undergo reduction to the dianions $[Ru_6C(CO)_{13}(\text{arene})]^{2-}$, which react further with the dication $[Ru(C_6H_6)(MeCN)_3]^{2+}$ to produce $[Ru_6C(CO)_{11}(\eta^6\text{-arene})(\mu_3\text{:}\eta^2\text{:}\eta^2\text{:}\eta^2\text{-}C_6H_6)]$.[2] This reaction was unexpected since interaction of the two ionic species was expected to yield a Ru_7C cluster.

We now wish to report the results of an extensive study of this chemistry. A new synthetic route to bis(arene) clusters has been devised, and the new compounds $[Ru_6C(CO)_{12}(\eta^6\text{-}1,3,5\text{-}C_6H_3Me_3)(\eta^4\text{-}C_6H_8)]$ (**2**), $[Ru_6C(CO)_{11}(\eta^6\text{-}1,3,5\text{-}C_6H_3Me_3)(\mu_3\text{:}\eta^2\text{:}\eta^2\text{:}\eta^2\text{-}C_6H_6)]$ (**3**), $[Ru_6C(CO)_{11}(\eta^6\text{-}1,3,5\text{-}C_6H_3Me_3)(\eta^6\text{-}C_6H_6)]$ (**4**), $[Ru_6C(CO)_{12}(\eta^6\text{-}1,3,5\text{-}C_6H_3Me_3)(\eta^4\text{-}1,3,5\text{-}C_6H_5Me_3)]$ (**5**), and $[Ru_6C(CO)_{11}(\eta^6\text{-}1,3,5\text{-}C_6H_3Me_3)_2]$ (**6**) have been prepared and fully characterized. The solid-state structure of the mixed benzene–mesitylene complex **4** and of the bis(mesitylene) species **6**, as well as their molecular organization in the crystal lattice, have been investigated by means of X-ray diffraction and packing potential energy calculations. Part of this work has been the subject of a preliminary report.[3]

The only other bis(arene) cluster characterized to date is $[Ru_6C(CO)_{11}(\eta^6\text{-}C_6H_6)(\mu_3\text{:}\eta^2\text{:}\eta^2\text{:}\eta^2\text{-}C_6H_6)]$, which contains two benzene moieties each bonded in a different manner, viz. one capping a triangular face of the metal octahedron and one terminally bound to an octahedral apex.[2] More recently, we have found that the face-capped square-pyramidal cluster $[Ru_5C(CO)_{12}(\mu_3\text{:}\eta^2\text{:}\eta^2\text{:}\eta^2\text{-}C_6H_6)]$ isomerizes on warming to the species $[Ru_5C(CO)_{12}(\eta^6\text{-}C_6H_6)]$ in which the benzene fragment is terminally bound to a basal Ru atom.[4] Remarkably, both isomers could be isolated and structurally characterized in the solid state. Furthermore, the investigation of the crystal structures of some of these carbonyl–arene clusters has afforded insight into the factors controlling the reorientational motion of the arene fragments in the solid state.[5] It has also been shown that precise relationships exist between the shape of the arene fragments and the molecular organization within the solid lattice.[6] In the case of $[Ru_6C(CO)_{11}(\eta^6\text{-}C_6H_6)(\mu_3\text{:}\eta^2\text{:}\eta^2\text{:}\eta^2\text{-}C_6H_6)]$, in particular, we have found that the two benzene fragments establish graphitic-like interactions throughout the crystal lattice.[6] This packing pattern has been related to the preference of the flat

(1) (a) Johnson, B. F. G.; Johnston, R. D.; Lewis, J. *J. Chem. Soc., Chem. Commun.* **1967**, 1057. (b) Johnson, B. F. G.; Johnston, R. D.; Lewis, J. *J. Chem. Soc. A* **1968**, 2865. (c) Mason, R.; Robinson, W. R. *J. Chem. Soc., Chem. Commun.* **1968**, 468.

(2) Gomez-Sal, M. P.; Johnson, B. F. G.; Lewis, J.; Raithby, P. R.; Wright, A. H. *J. Chem. Soc., Chem. Commun.* **1985**, 1682.

(3) Braga, D.; Grepioni, F.; Righi, S.; Dyson, P. J.; Johnson, B. F. G.; Lewis, J.; Bailey, P. J.; Martinelli, M. *J. Chem. Soc., Dalton Trans.* **1992**, 2121.

(4) Bailey, P. J.; Braga, D.; Dyson, P. J.; Grepioni, F.; Johnson, B. F. G.; Lewis, J.; Sabatino, P. *J. Chem. Soc., Chem. Commun.* **1992**, 177.

(5) (a) Braga, D.; Grepioni, F.; Johnson, B. F. G.; Lewis, J.; Martinelli, M. *J. Chem. Soc., Dalton Trans.* **1990**, 1847. (b) Braga, D.; Grepioni, F.; Johnson, B. F. G.; Lewis, J.; Housecroft, C. E.; Martinelli, M. *Organometallics* **1991**, *10*, 1260.

(6) Braga, D.; Grepioni, F.; Johnson, B. F. G.; Chen, H.; Lewis, J. *J. Chem. Soc., Dalton Trans.* **1991**, 2559.

0276-7333/92/2311-4042$03.00/0

Scheme I. Synthesis of Mixed-Arene Hexaruthenium Carbide Carbonyl Complexes[a]

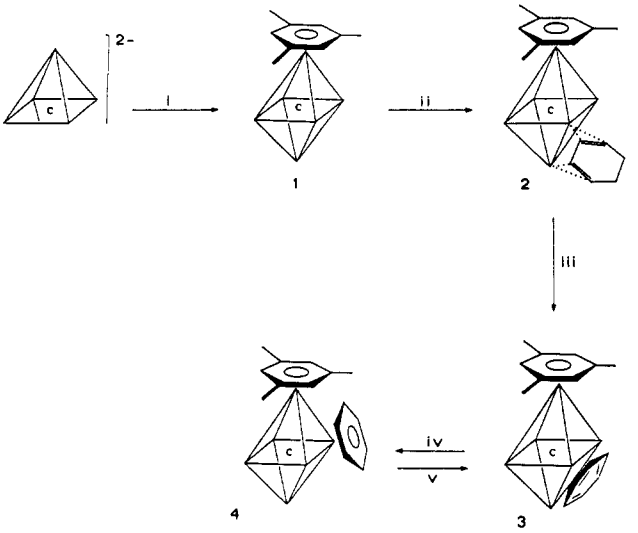

[a] Reagents and conditions: (i) dropwise addition of $[Ru_5C(CO)_{14}]^{2-}$ into a refluxing CH_2Cl_2 solution of $[Ru(C_6H_3Me_3)(PhCN)]^{2+}$; (ii) Me_3NO/CH_2Cl_2 added dropwise to a CH_2Cl_2/1,3-cyclohexadiene solution; (iii) Me_3NO/CH_2Cl_2 added dropwise to a CH_2Cl_2 solution; (iv) allow CH_2Cl_2 solution to stand at −20 °C for 10–15 weeks; (v) refluxing hexane.

benzene fragments belonging to neighboring molecules on one side and of the carbonyl groups on the other to associate separately in the lattice. Hence, a further aim of this study has been to investigate whether or not this packing preference is transferable from crystal to crystal on changing either the arene or its coordination mode.

Results and Discussion

Synthesis and Chemical Characterization. The pentaruthenium dianion $[Ru_5C(CO)_{14}]^{2-}$ reacts with $[Ru(C_6H_3Me_3)(PhCN)_3]^{2+}$ in dichloromethane to yield the previously reported derivative $[Ru_6C(CO)_{14}(\eta^6\text{-}1,3,5\text{-}C_6H_3Me_3)]$ (**1**) in good yield. We find that this route is preferable to that reported earlier[1] in that a single product is obtained in higher yield. Treatment of **1** with 2 equiv of Me_3NO in dichloromethane in the presence of 1,3-cyclohexadiene gives the cluster compound $[Ru_6C(CO)_{12}(\eta^6\text{-}1,3,5\text{-}C_6H_3Me_3)(\eta^4\text{-}C_6H_8)]$ (**2**) in moderate yield. Further reaction of **2** with Me_3NO in dichloromethane brings about the formation of the bis(arene) complex $[Ru_6C(CO)_{11}(\eta^6\text{-}1,3,5\text{-}C_6H_3Me_3)(\mu_3\text{:}\eta^2\text{:}\eta^2\text{:}\eta^2\text{-}C_6H_6)]$ (**3**). In this reaction, we presume that compound **2** is first "activated" by the oxidation of a coordinated CO to CO_2 by Me_3NO thus generating the coordinatively unsaturated intermediate $[Ru_6C(CO)_{11}(\eta^6\text{-}1,3,5\text{-}C_6H_3Me_3)(\eta^4\text{-}C_6H_8)]$. This step is then followed by oxidative cleavage of a C–H bond to generate a dienyl compound, as yet unobserved, which undergoes a second similar C–H bond cleavage to produce the required product **3** and, presumably, dihydrogen. On standing, complex **3** undergoes reversible isomerization to $[Ru_6C(CO)_{11}(\eta^6\text{-}1,3,5\text{-}C_6H_3Me_3)(\eta^6\text{-}C_6H_6)]$ (**4**), which has been fully characterized by single-crystal X-ray diffraction (see below). By similar routes the complexes $[Ru_6C(CO)_{12}(\eta^6\text{-}1,3,5\text{-}C_6H_3Me_3)(\eta^4\text{-}1,3,5\text{-}C_6H_5Me_3)]$ (**5**) and $[Ru_6C(CO)_{11}(\eta^6\text{-}1,3,5\text{-}C_6H_3Me_3)_2]$ (**6**) have been prepared (see Scheme I). The molecular structure of **6** has also been determined by single-crystal X-ray diffraction.

Molecular Structure of *cis*-$[Ru_6C(CO)_{11}(\eta^6\text{-}1,3,5\text{-}C_6H_3Me_3)(\eta^6\text{-}C_6H_6)]$ (4) and *trans*-$[Ru_6C(CO)_{11}(\eta^6\text{-}1,3,5\text{-}C_6H_3Me_3)_2]$ (6) in the Solid State. The solid-state molecular structure of **4** is shown in Figure 1a together with

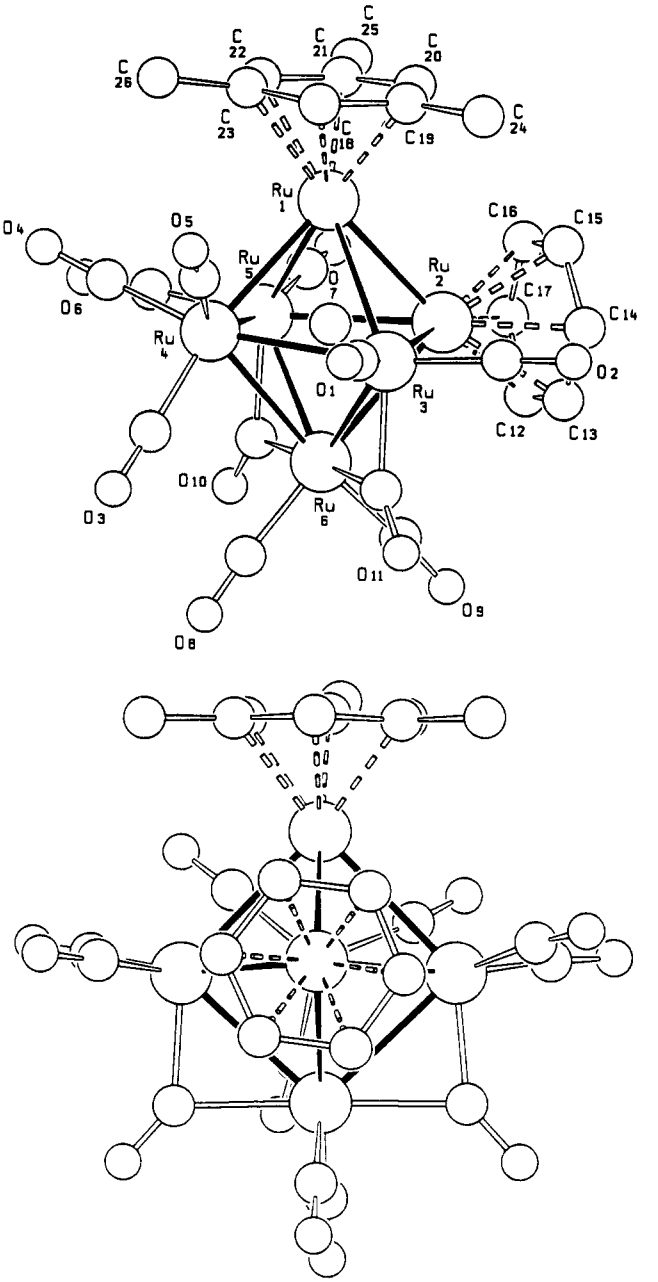

Figure 1. (a) Top: Molecular structure of **4**, showing the labeling scheme. The C atoms of the CO groups bear the same numbering as the corresponding O atoms. H atoms of the mesitylene and benzene ligands are omitted for clarity. (b) Bottom: Alternative view of the structure of **4**, showing the *pseudo-m*-symmetry.

the atomic labeling scheme. Relevant structural parameters are listed in Table I. The metal atom framework is constituted of a Ru_6 octahedron encapsulating a C(carbide) atom. This cluster is unique on two counts. First, it contains two different arene fragments (mesitylene and benzene) both coordinated in a terminal fashion, and second, the two unsaturated ligands occupy two contiguous sites over the metal framework. The two ruthenium atoms bearing the arene ligands do not carry any CO ligand. Two of the 13 CO ligands are in asymmetric bridging positions along two consecutive edges of the octahedral core, while the remaining CO ligands are terminally bound. The terminal ligands, however, show a complex pattern of Ru–C–O bending due to the presence of the two bulky arene fragments next to each other over the metal frame. It is remarkable that the two arenes have chosen to adopt the highly crowded cis location, while occupation of op-

Table I. Relevant Bond Distances (Å) and Bond Angles (deg) for $Ru_6C(CO)_{11}(\eta^6\text{-}1,3,5\text{-}C_6H_3Me_3)(\eta^6\text{-}C_6H_6)$ (4)

Ru(2)–Ru(1)	2.837 (2)	Ru(3)–Ru(1)	3.013 (2)
Ru(4)–Ru(1)	2.816 (2)	Ru(5)–Ru(1)	2.960 (2)
Ru(3)–Ru(2)	2.872 (2)	Ru(5)–Ru(2)	2.998 (2)
Ru(6)–Ru(2)	2.900 (2)	Ru(4)–Ru(3)	2.860 (2)
Ru(6)–Ru(3)	2.850 (2)	Ru(5)–Ru(4)	2.920 (2)
Ru(6)–Ru(4)	2.972 (2)	Ru(6)–Ru(5)	2.831 (2)
C(99)–Ru(1)	1.95 (1)	C(99)–Ru(2)	1.93 (1)
C(99)–Ru(3)	2.07 (1)	C(99)–Ru(4)	2.11 (1)
C(99)–Ru(5)	2.08 (1)	C(99)–Ru(6)	2.17 (1)
Ru(1)–C(18)	2.22 (1)	C(21)–C(22)	1.38 (2)
Ru(1)–C(19)	2.24 (1)	C(22)–C(23)	1.44 (3)
Ru(1)–C(20)	2.24 (1)	C(23)–C(18)	1.40 (3)
Ru(1)–C(21)	2.24 (1)	C(19)–C(24)	1.49 (3)
Ru(1)–C(22)	2.24 (1)	C(21)–C(25)	1.51 (3)
Ru(1)–C(23)	2.31 (1)	C(23)–C(26)	1.50 (3)
		C(18)–C(19)	1.42 (3)
		C(19)–C(20)	1.43 (3)
		C(20)–C(21)	1.43 (3)
Ru(2)–C(12)	2.25 (1)	C(12)–C(13)	1.38 (3)
Ru(2)–C(13)	2.22 (1)	C(13)–C(14)	1.36 (3)
Ru(2)–C(14)	2.24 (1)	C(14)–C(15)	1.43 (3)
Ru(2)–C(15)	2.20 (1)	C(15)–C(16)	1.36 (3)
Ru(2)–C(16)	2.22 (1)	C(16)–C(17)	1.36 (3)
Ru(2)–C(17)	2.25 (1)	C(17)–C(12)	1.38 (3)
Ru(3)–C(1)	1.86 (1)	Ru(3)–C(2)	1.84 (1)
Ru(3)–C(11)	2.00 (1)	Ru(4)–C(3)	1.90 (1)
Ru(4)–C(4)	1.90 (1)	Ru(4)–C(5)	1.90 (1)
Ru(5)–C(6)	1.90 (1)	Ru(5)–C(7)	1.90 (1)
Ru(5)–C(10)	1.98 (1)	Ru(6)–C(8)	1.89 (1)
Ru(6)–C(9)	1.87 (1)	Ru(6)–C(10)	2.20 (1)
Ru(6)–C(11)	2.20 (1)	C(1)–O(1)	1.13 (1)
C(2)–O(2)	1.18 (1)	C(3)–O(3)	1.14 (1)
C(4)–O(4)	1.13 (1)	C(5)–O(5)	1.13 (1)
C(6)–O(6)	1.15 (1)	C(7)–O(7)	1.14 (1)
C(8)–O(8)	1.13 (1)	C(9)–O(9)	1.14 (1)
C(10)–O(10)	1.19 (1)	C(11)–O(11)	1.16 (1)
Ru(3)–C(1)–O(1)	177 (1)	Ru(3)–C(2)–O(2)	175 (1)
Ru(4)–C(3)–O(3)	174 (2)	Ru(4)–C(4)–O(4)	173 (1)
Ru(4)–C(5)–O(5)	176 (1)	Ru(5)–C(6)–O(6)	173 (1)
Ru(5)–C(7)–O(7)	175 (1)	Ru(6)–C(8)–O(8)	176 (1)
Ru(6)–C(9)–O(9)	177 (1)	Ru(5)–C(10)–O(10)	143 (1)
Ru(6)–C(10)–O(10)	132 (1)	Ru(3)–C(11)–O(11)	142 (1)
Ru(6)–C(11)–O(11)	133 (1)		
C(17)–C(12)–C(13)	118 (1)	C(14)–C(13)–C(12)	122 (1)
C(15)–C(14)–C(13)	118 (1)	C(16)–C(15)–C(14)	121 (1)
C(17)–C(16)–C(15)	119 (1)	C(16)–C(17)–C(12)	122 (1)
C(19)–C(18)–C(19)	123 (1)	C(20)–C(19)–C(18)	116 (1)
C(21)–C(20)–C(19)	123 (1)	C(22)–C(21)–C(20)	117 (1)
C(23)–C(22)–C(21)	123 (1)	C(22)–C(23)–C(18)	118 (1)

posite sites as in *trans*-$[Ru_6C(CO)_{11}(\eta^6\text{-}1,3,5\text{-}C_6H_3Me_3)_2]$ (see below) would have, most certainly, reduced the interarene interactions. Figure 1b shows that the torsions of the two arenes and of the tricarbonyl unit opposite to benzene represent the most significant deviations from idealized *m*-symmetry, with the pseudo-mirror plane relating the two bridging CO's and ideally bisecting the mesitylene and benzene fragments. The possible role played by crystal packing optimization in determining this structural choice will be discussed later on.

Metal–metal bonds fall in the range 2.816 (2)–3.013 (2) Å; the bond between the two ruthenium atoms bearing the two arenes is one of the shortest in the structure [Ru(1)–Ru(2) = 2.837 (2) Å], while the longest one [Ru(1)–Ru(3) = 3.013 (2) Å] involves the ruthenium atom bearing mesitylene and a neighboring CO-bridged ruthenium atom.

As previously noted in other Ru_6–arene clusters,[6] the C(carbide) atom in **4** is offset with respect to the center of the octahedral cavity, being closer to the arene-bound ruthenium atoms [Ru(1)–C(99) = 1.95 (1), Ru(2)–C(99) = 1.93 (1) Å] than to the other atoms of the cluster [range 2.07–2.17 (1) Å]. C–C distances within the two aromatic rings fall in the ranges 1.38 (2)–1.44 (2) and 1.36 (2)–1.43 (3) Å for mesitylene and benzene, respectively, with no recognizable pattern of bond length alternation. The two aromatic fragments are essentially planar (maximum deviation from the least-squares planes of the C_6 rings of 0.04 Å), while the methyl group eclipsed over Ru(4) is pushed slightly above the ring plane [C(28) elevation 0.21 Å]. The two arene planes form an angle of 89.8°. Ru–C(mesitylene) distances are only slightly longer in their mean values than the Ru–C(benzene) ones [2.25 (1) versus 2.23 (1) Å]. These values are strictly comparable with those observed in other Ru_6C clusters containing η^6-arene fragments.[6]

Table II. Relevant Bond Distances (Å) and Bond Angles (deg) for $Ru_6C(CO)_{11}(\eta^6\text{-}1,3,5\text{-}C_6H_3Me_3)_2$ (6)

Ru(1)–Ru(3)	3.089 (1)	Ru(1)–C(99)	2.05 (1)
Ru(1)–Ru(4)	2.796 (1)	Ru(2)–C(99)	2.09 (1)
Ru(1)–Ru(5)	2.865 (1)	Ru(3)–C(99)	2.06 (1)
Ru(1)–Ru(6)	2.865 (1)	Ru(4)–C(99)	2.06 (1)
Ru(2)–Ru(3)	2.871 (1)	Ru(5)–C(99)	1.96 (1)
Ru(2)–Ru(4)	2.917 (1)	Ru(6)–C(99)	1.98 (1)
Ru(2)–Ru(6)	2.853 (1)	Ru(5)–C(12)	2.27 (1)
Ru(3)–Ru(5)	2.838 (1)	Ru(5)–C(13)	2.28 (1)
Ru(3)–Ru(6)	2.842 (1)	Ru(5)–C(14)	2.22 (1)
Ru(4)–Ru(5)	2.857 (1)	Ru(5)–C(15)	2.27 (1)
Ru(4)–Ru(6)	2.876 (1)	Ru(5)–C(16)	2.25 (1)
Ru(2)–Ru(5)	2.848 (1)	Ru(5)–C(17)	2.25 (1)
Ru(6)–C(21)	2.23 (1)	Ru(6)–C(22)	2.27 (1)
Ru(6)–C(23)	2.25 (1)	Ru(6)–C(26)	2.27 (1)
Ru(6)–C(24)	2.25 (1)	Ru(6)–C(25)	2.27 (1)
Ru(2)–C(6)	2.06 (1)	Ru(3)–C(6)	2.08 (1)
C(6)–O(6)	1.17 (1)	Ru(4)–C(8)	1.91 (1)
C(8)–O(8)	1.13 (1)	Ru(2)···C(8)	2.78
Ru(4)–C(8)–O(8)	165.2 (6)		
Ru–Ru(av)	2.876 (1)		
Ru–C(av)	1.89 (1)		
C–O(av)	1.13 (1)		
C(12)–C(13)	1.41 (1)	C(17)–C(12)–C(13)	121.5 (6)
C(13)–C(14)	1.42 (1)	C(14)–C(13)–C(12)	118.3 (6)
C(14)–C(15)	1.42 (1)	C(13)–C(14)–C(15)	121.0 (6)
C(15)–C(16)	1.38 (1)	C(14)–C(15)–C(16)	119.1 (6)
C(16)–C(17)	1.43 (1)	C(15)–C(16)–C(17)	121.9 (6)
C(17)–C(12)	1.41 (1)	C(16)–C(17)–C(12)	118.0 (6)
C(21)–C(22)	1.42 (1)	C(26)–C(21)–C(22)	120.2 (6)
C(22)–C(23)	1.42 (1)	C(21)–C(22)–C(23)	118.1 (6)
C(23)–C(24)	1.41 (1)	C(22)–C(23)–C(24)	121.7 (6)
C(24)–C(25)	1.39 (1)	C(23)–C(24)–C(25)	118.8 (6)
C(25)–C(26)	1.40 (1)	C(24)–C(25)–C(26)	121.4 (6)
C(26)–C(21)	1.41 (1)	C(25)–C(26)–C(21)	119.7 (6)

The two asymmetric bridging CO's show their longer Ru–C distances from the same ruthenium atom [Ru(6)–C(10) = 2.20 (2), Ru(6)–C(11) = 2.20 (2) Å], this being the only ruthenium atom involved in bonding with four CO ligands.

The structure of *trans*-$[Ru_6C(CO)_{11}(\eta^6\text{-}1,3,5\text{-}C_6H_3Me_3)_2]$ (**6**) is shown in Figure 2a together with the labeling scheme. Relevant bond lengths and angles are listed in Table II. The octahedral metal cluster is sandwiched between the two terminally bound mesitylene ligands, which adopt an almost exact eclipsed conformation (see Figure 2b). Ru–Ru bond distances range from 2.796 (1) to 3.089 (1) Å. The mesitylene ligands are η^6-bound to two opposite Ru atoms of the octahedral framework [mean Ru–C distance 2.26 (1) Å]. The planes of the two aromatic rings form angles of 5.6° [C(21)–C(26)] and 4.4° [C(12)–C(17)] with respect to the molecular equatorial plane. Expectedly, the methyl groups on both fragments are pushed slightly above the C_6-ring planes.

As discussed above for **4**, Ru–C(carbide) distances involving the two substituted Ru atoms [Ru(5)–C = 1.96 (1), Ru(6)–C = 1.98 (1) Å] are appreciably shorter than those

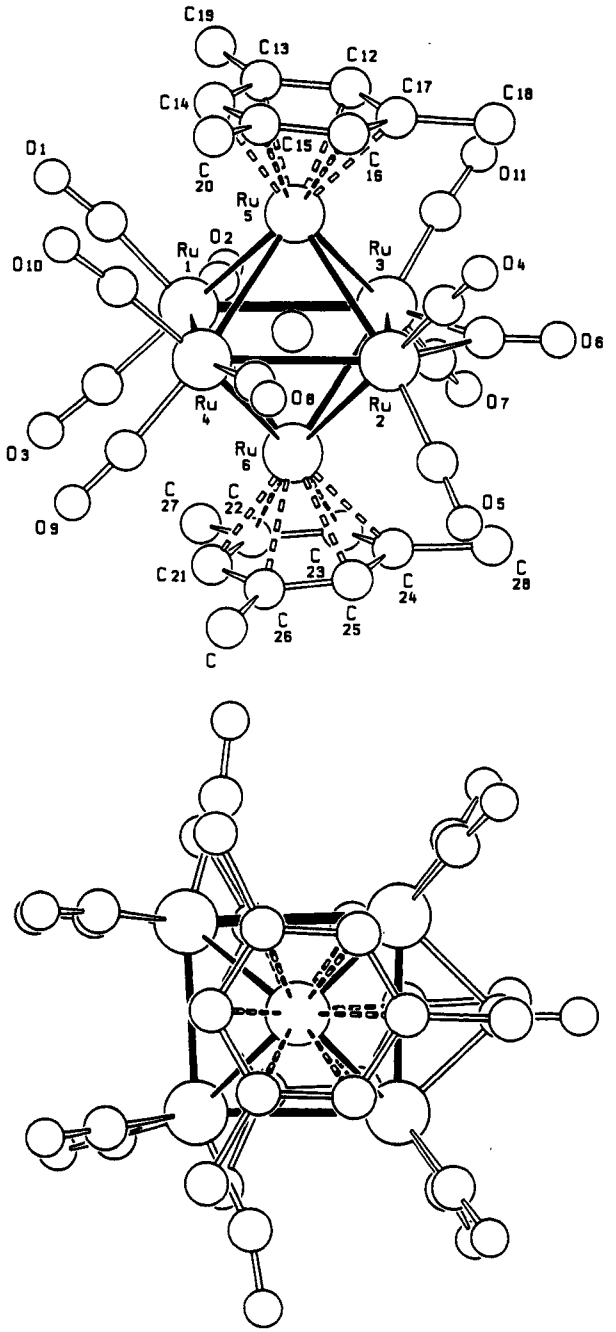

Figure 2. (a) Top: Molecular structure of **6**, showing the labeling scheme. The C atoms of the CO groups bear the same numbering as the corresponding O atoms. H atoms of the mesitylene groups are omitted for clarity. (b) Botton: Alternative view of the structure of **6**, showing the eclipsed conformation of the two mesitylene rings.

involving the equatorial Ru atoms [range 2.06 (1)–2.08 (1) Å] so that the octahedral framework is "squeezed" along the mesitylene-cluster coordination axis. The CO-ligand distribution on the equatorial atoms recalls that observed in $[Ru_6C(CO)_{17}]$,[7] i.e. one bridging ligand, and two semibridging CO's lie in the equatorial plane, while eight terminal ligands are distributed above and below the plane.

Structure of the Crystals of 4 and 6. We have recently discovered,[6] upon reinvestigation of the crystal

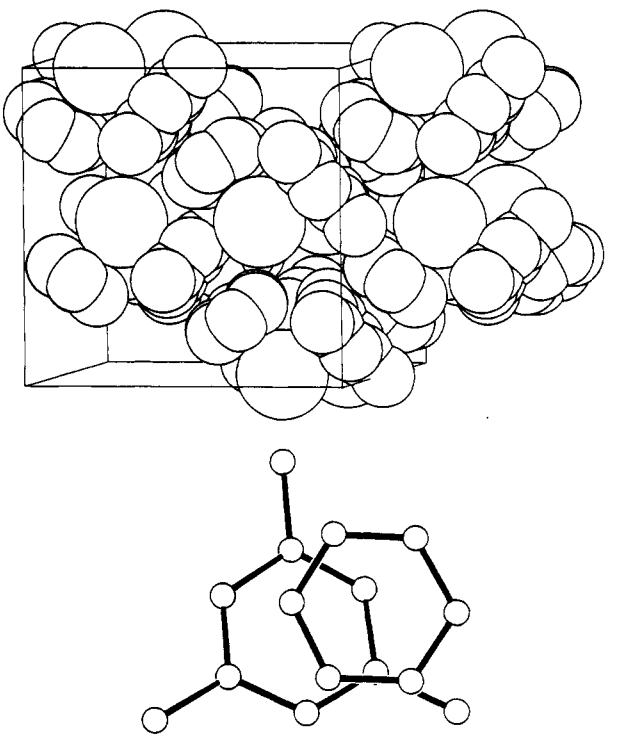

Figure 3. (a) Top: Molecular organization in crystalline **4**. The mesitylene and benzene ligands of neighboring molecules face each other throughout the lattice, forming "snakelike" molecular chains in the 010 lattice direction (cluster frames and CO ligands are represented by large spheres). (b) Botton: Projection perpendicular to the benzene plane of the benzene–mesitylene graphitic-like interaction.

structure of the bis(benzene) derivative $[Ru_6C(CO)_{11}(\eta^6\text{-}C_6H_6)(\mu_3\text{-}\eta^2\text{:}\eta^2\text{:}\eta^2\text{-}C_6H_6)]$ that the two benzene fragments establish graphitic-like interactions in the lattice, generating "snakelike" molecular rows along the 011 lattice direction in the triclinic cell. This packing pattern could be decoded by means of approximate packing potential energy calculations (see below for a brief description of the method), which we have now applied to the investigation of the crystal structures of **4** and **6**. We have found that the tendency to group together the arene fragments and to establish preferential arene–arene intermolecular interactions observed in crystalline $[Ru_6C(CO)_{11}(\eta^6\text{-}C_6H_6)(\mu_3\text{-}\eta^2\text{:}\eta^2\text{:}\eta^2\text{-}C_6H_6)]$ is maintained in crystalline **4** and **6**. This is particularly remarkable in view of the differences in arene type, in coordination mode, and in overall molecular geometry between the three species.

In crystalline **4** the benzene and mesitylene ligands belonging to the reference molecule (RM; see below) are almost face-to-face with, respectively, the mesitylene and benzene ligands belonging to next-neighboring molecules, as shown in Figure 3a. These molecular "snakes" extend along the *b*-direction. Figure 3b shows a projection of one mesitylene–benzene pair perpendicular to the plane defined by this latter ligand.

In a manner analogous to crystalline **4**, the mesitylene fragments in crystalline **6** are paired throughout the lattice as sketched in Figure 4a. Each molecule is related to the next along the snake by a crystallographic center of symmetry. The distance between the arene planes is ca. 3.6 Å, i.e. only slightly longer than in graphite itself. A projection of the two mesitylene–mesitylene interactions (Figure 4b) clearly shows the different pairing of the ligands on the two sides of the reference molecule.

There is, therefore, a cluster tendency to place the arene fragments together in the lattice. With the mono(arene)

(7) Sirigu, A.; Bianchi, M.; Benedetti, E. *J. Chem. Soc., Chem. Commun.* **1969**, 596. For a recent redetermination on two polymorphic modifications, see also: Braga, D.; Grepioni, F.; Dyson, P. J.; Johnson, B. F. G.; Frediani, P.; Bianchi, M.; Piacenti, F. *J. Chem. Soc., Dalton Trans.* **1992**, 2565.

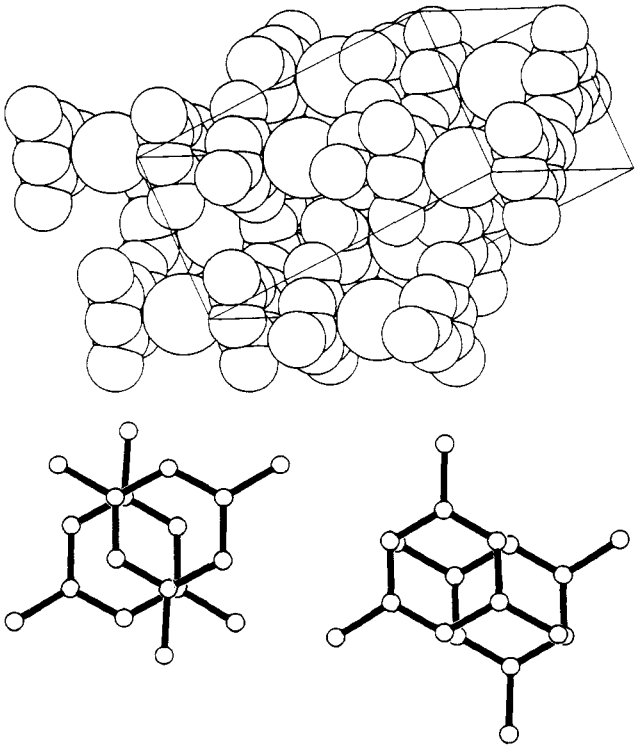

Figure 4. (a) Top: Molecular organization in crystalline **6**. The two mesitylene ligands form graphitic-like interactions in the 101 lattice direction (cluster frames and CO ligands are represented by large spheres). (b) Botton: Comparison of the two different types of mesitylene–mesitylene intermolecular interactions in crystalline **6**.

derivatives this is achieved by forming arene ribbons or layers through the lattice,[6] while with bis(arenes) this is better achieved by placing the ligands face to face. This general behavior confirms our previous hypothesis on the factors governing the packing choice with arene clusters: the most efficient way to pack together molecules containing *both* arenes and CO ligands is to group together the flat arene fragments on one side and the CO ligands protruding from the cluster surface on the other. In this way optimum CO···CO interlocking is preserved.

The reason for the adoption of the cis-η^6-coordination when the arenes are benzene and mesitylene as in **4**, while two mesitylene ligands are trans-η^6-coordinated in **6**, is difficult to understand. While we recognize the subtle balance between steric, electronic, and packing effects, it is worth noting that the cis coordination is four times as probable as the trans coordination (given that the precursor contains a η^6-coordinated mesitylene ligand). The trans coordination, on the other hand, is certainly favored if the second light is another sterically demanding mesitylene fragment. It also seems possible that, while the η^6-bonding of mesitylene minimizes intramolecular interactions with CO groups, face-capping decreases the electronic perturbation of the whole cluster orbital system upon substitution of three CO's. It would appear that formation of the face-capped cluster is under kinetic control, probably because of the initial η^4-coordination of the cyclohexadienyl ligand, and this product then evolves to the more thermodynamically stable terminal product.

Experimental Section

All reactions were carried out with the exclusion of air using solvents dried by conventional methods. Subsequent workup of products was carried out without precautions to exclude air. Infrared spectra were recorded on a Perkin-Elmer 1600 Series FTIR in CH_2Cl_2 using NaCl cells (0.5-mm path length). Fast atom bombardment mass spectra were obtained on a Kratos MS50TC using CsI as a calibrant. NMR spectra were recorded in $CDCl_3$ using Brucker WP200 and AM360 instruments, calibrated with TMS. Products were separated by thin-layer chromatography (TLC) on plates supplied by Merck with a 0.25-mm layer of Kieselgel 60 F_{254} using hexane (70%)/dichloromethane (30%) as eluant. $[Ru_5C(CO)_{14}]^{2-}$ and $[Ru(C_6H_3Me_3)(PhCN)_3]^{2+}$ were prepared by the literature methods.[8] Trimethylamine *N*-oxide was sublimed directly before use.

Table III. Crystal Data and Details of Measurements for Compounds 4 and 6

formula	$C_{27}H_{18}O_{11}Ru_6$	$C_{30}H_{24}O_{11}Ru_6$
M_r	1124.6	1166.7
cryst size (mm)	0.10 × 0.12 × 0.11	0.14 × 0.12 × 0.15
system	orthorhombic	monoclinic
space group	*Pbca*	$P2_1/c$
a (Å)	15.996 (5)	10.084 (1)
b (Å)	15.997 (5)	16.984 (3)
c (Å)	23.81 (1)	19.425 (5)
β (deg)		88.94 (1)
V (Å^3)	6093.7	3326.4
Z	8	4
$F(000)$	4256	2224
D_{calcd} (g·cm^{-3})	2.45	2.33
λ(Mo Kα) (Å)	0.710 69	0.710 69
μ(Mo Kα) (cm^{-1})	26.87	24.63
θ range (deg)	2.5–25	2.5–25
scan mode	$\omega/2\theta$	$\omega/2\theta$
ω-scan width (deg)	0.60	0.80
requested counting $\sigma(I)/I$	0.02	0.02
prescan rate (deg min^{-1})	5	6
prescan acceptance $\sigma(I)/I$	0.5	0.5
max scan time (s)	90	100
no. of measd reflcns	5896	6231
no. of unique obsd reflcns used in the refinement [$I > 2.0\sigma(I)$]	1728	4437
no. of refined params	324	431
R, R_w,[a]	0.035, 0.033	0.032, 0.035
S[b]	1.2	1.3
k, g	1.51, 0.000 47	1.19, 0.000 87

[a] $R_w = \sum[(F_o - F_c)w^{1/2}]/\sum F_o w^{1/2})$, where $w = k/[\sigma(F) + |g|F^2]$. [b] $S = \{\sum_N[w(F_o - F_c)^2]/(N_{obs} - N_{var})\}^{1/2}$.

Reaction of $[Ru_6C(CO)_{14}(\eta^6\text{-}1,3,5\text{-}C_6H_3Me_3)]$ with 1,3,5-$C_6H_5Me_3$ and 1,3-C_6H_8. (i) An excess of 1,3,5-trimethyl-2,4-cyclohexadiene (1 mL) was added to a solution of $[Ru_6C(CO)_{14}(\eta^6\text{-}1,3,5\text{-}C_6H_3Me_3)]$ (50 mg) in CH_2Cl_2 (50 mL). A solution of Me_3NO (11 mg, 3 mol equiv) in CH_2Cl_2 (5 mL) was added dropwise. The mixture was stirred for 45 min at room temperature and the reaction monitored by IR spectroscopy, ensuring complete conversion of the starting material. The solvent was removed in vacuo and the product obtained by TLC. The brown band was extracted and characterized by spectroscopy to be $[Ru_6C(CO)_{11}(\eta^6\text{-}1,3,5\text{-}C_6H_3Me_3)_2]$ (8 mg). Spectroscopic data for $[Ru_6C(CO)_{11}(\eta^6\text{-}1,3,5\text{-}C_6H_3Me_3)_2]$ are as follows. IR (CH_2Cl_2): 2035 (m), 1994 (vs), 1972 (s), 1934 (m), 1793 (w, br) cm^{-1}. ^{1}H NMR (CD_2Cl_2): δ 5.29 (s, 1H), 2.17 (s, 3H). EI mass spectrum: M$^+$, m/e 1167 (calculated m/e 1167). Anal. Calcd: C, 30.87; H, 2.06. Found: C, 30.71; H, 2.28.

(ii) Me_3NO (5 mg, 2.1 mol equiv) in CH_2Cl_2 (5 mL) was added dropwise to a solution of $[Ru_6C(CO)_{14}[\eta^6\text{-}1,3,5\text{-}C_6H_3Me_3)]$ (35 mg) in CH_2Cl_2 containing an excess of 1,3-cyclohexadiene (1 mL). The consumption of starting material was monitored by IR spectroscopy, and after the mixture was stirred for 20 min at room temperature no starting material remained. The solvent was removed in vacuo and the product isolated by TLC. The brown band was extracted and characterized by spectroscopy to be $[Ru_6C(CO)_{12}(\eta^6\text{-}1,3,5\text{-}C_6H_3Me_3)(\eta^4\text{-}C_6H_8)]$ (10 mg). Spectroscopic data are as follows. IR (CH_2Cl_2): 2041 (m), 1998 (vs), 1960 (vw, br), 1814 (vw, br). ^{1}H NMR ($CDCl_3$): δ 5.34 (s, 3H), 4.88 (t, 1H), 4.86 (t, 1H), 4.15 (t, 1H), 3.52 (t, 1H), 2.30 (s, 9H), 2.12 (m, 1H), 2.05 (m, 1H), 1.03 (m, 1H), 0.86 (m, 1H). EI mass spectrum: m/e 1144 (calculated m/e 1144). Anal. Calcd: C, 29.12; H, 1.73. Found: C 28.88; H, 1.87.

(8) Bennet, M. A.; Smith, A. K. *J. Chem. Soc., Dalton Trans*, **1974**, 233.

Table IV. Fractional Atomic Coordinates for 4

atom	x	y	z
Ru(1)	0.07715 (8)	0.31445 (8)	0.12181 (6)
Ru(2)	0.10617 (9)	0.14050 (8)	0.13443 (6)
Ru(3)	−0.01523 (9)	0.21328 (8)	0.20868 (6)
Ru(4)	−0.09634 (9)	0.28715 (8)	0.11383 (6)
Ru(5)	0.01252 (9)	0.19556 (9)	0.03702 (6)
Ru(6)	−0.07037 (9)	0.10356 (8)	0.12194 (7)
C(99)	0.0109 (9)	0.2123 (9)	0.1237 (6)
C(1)	−0.0744 (12)	0.2784 (11)	0.2599 (8)
O(1)	−0.1092 (9)	0.3155 (8)	0.2928 (6)
C(2)	0.0507 (14)	0.1800 (13)	0.2681 (9)
O(2)	0.0882 (11)	0.1603 (11)	0.3086 (6)
C(3)	−0.2102 (14)	0.2544 (13)	0.1208 (10)
O(3)	−0.2791 (10)	0.2406 (11)	0.1277 (9)
C(4)	−0.1196 (10)	0.3499 (10)	0.0481 (7)
O(4)	−0.1352 (10)	0.3934 (9)	0.0125 (6)
C(5)	−0.1103 (13)	0.3803 (12)	0.1618 (8)
O(5)	−0.1228 (9)	0.4347 (9)	0.1909 (5)
C(6)	−0.0335 (14)	0.2438 (12)	−0.0288 (7)
O(6)	−0.0586 (10)	0.2658 (9)	−0.0715 (6)
C(7)	0.1062 (13)	0.1636 (11)	−0.0063 (7)
O(7)	0.1592 (8)	0.1389 (9)	−0.0336 (6)
C(8)	−0.1835 (13)	0.0724 (12)	0.1121 (8)
O(8)	−0.2501 (9)	0.0505 (10)	0.1081 (7)
C(9)	−0.0458 (10)	−0.0096 (11)	0.1317 (8)
O(9)	−0.0339 (9)	−0.0794 (8)	0.1372 (7)
C(10)	−0.0556 (11)	0.0925 (11)	0.0304 (8)
O(10)	−0.0829 (8)	0.0441 (7)	−0.0029 (5)
C(11)	−0.0917 (11)	0.1142 (9)	0.2130 (7)
O(11)	−0.1288 (10)	0.0743 (8)	0.2448 (6)
C(12)	0.1497 (11)	0.0077 (11)	0.1221 (8)
C(13)	0.1449 (11)	0.0246 (11)	0.1787 (8)
C(14)	0.1876 (11)	0.0889 (12)	0.2024 (9)
C(15)	0.2355 (12)	0.1417 (13)	0.1662 (8)
C(16)	0.2397 (12)	0.1264 (12)	0.1101 (8)
C(17)	0.1988 (11)	0.0585 (12)	0.0892 (8)
C(18)	0.0923 (11)	0.4372 (11)	0.1641 (8)
C(19)	0.1621 (11)	0.3864 (11)	0.1785 (8)
C(20)	0.2102 (11)	0.3550 (11)	0.1324 (8)
C(21)	0.1865 (10)	0.3670 (10)	0.0752 (7)
C(22)	0.1185 (11)	0.4178 (10)	0.0649 (7)
C(23)	0.0717 (11)	0.4575 (11)	0.1088 (7)
C(24)	0.1847 (11)	0.3701 (11)	0.2381 (7)
C(25)	0.2377 (12)	0.3337 (12)	0.0267 (7)
C(26)	0.0048 (11)	0.5200 (12)	0.0946 (8)

Reaction of $[Ru_6C(CO)_{12}(\eta^6\text{-}1,3,5\text{-}C_6H_3Me_3)(\eta^4\text{-}C_6H_8)]$ with Me_3NO/CH_2Cl_2. Me_3NO (4 mg, 1.1 mol equiv) in CH_2Cl_2 (5 mL) was added dropwise to a solution of $[Ru_6C(CO)_{12}(\eta^6\text{-}1,3,5\text{-}C_6H_3Me_3)(\eta^4\text{-}C_6H_8)]$ (15 mg) in CH_2Cl_2 (25 mL). The mixture was stirred for 25 min at room temperature and the reaction monitored by IR spectroscopy, ensuring complete conversion of starting material. The solvent was removed in vacuo and the product purified by TLC. The red/brown band was extracted and characterized by spectroscopy as $[Ru_6C(CO)_{11}(\eta^6\text{-}1,3,5\text{-}C_6H_3Me_3)(\mu_3\text{-}\eta^2\text{:}\eta^2\text{:}\eta^2\text{-}C_6H_6)]$ (5 mg). Spectroscopic data are as follows. IR (CH_2Cl_2): 2034 (m), 1996 (vs), 1933 (w, br). ^1H NMR ($CDCl_3$): δ 5.55 (s, 3H), 4.09 (s, 6H), 2.29 (s, 9H). EI mass spectrum: m/e 1142 (calculated m/e 1144).

Isomerization of $[Ru_6C(CO)_{11}(\eta^6\text{-}1,3,5\text{-}C_6H_3Me_3)(\mu_3\text{-}\eta^2\text{:}\eta^2\text{:}\eta^2\text{-}C_6H_6)]$. $[Ru_6C(CO)_{11}(\eta^6\text{-}1,3,5\text{-}C_6H_3Me_3)(\mu_3\text{-}\eta^2\text{:}\eta^2\text{:}\eta^2\text{-}C_6H_6)]$ (6 mg) was dissolved in CH_2Cl_2 (20 mL). The solution was stoppered and stored at −20 °C for 10–15 weeks. IR spectroscopy indicated approximately 95% conversion of the starting material. Only one product was obtained from TLC, which was characterized by spectroscopy as $[Ru_6C(CO)_{11}(\eta^6\text{-}1,3,5\text{-}C_6H_3Me_3)(\eta^6\text{-}C_6H_6)]$. Spectroscopic data are as follows. IR (CH_2Cl_2): 2048 (m), 1996 (vs), 1948 (w, br). ^1H NMR ($CDCl_3$): δ 5.57 (s, 6H), 5.50 (s, 3H), 2.32 (s, 9H). EI mass spectrum: m/e 1142 (calculated m/e 1144). Anal. Calcd: C, 28.88; H, 1.60. Found: C, 28.69; H, 1.81.

Structural Characterization. The diffraction data for the species discussed herein were collected on an Enraf-Nonius CAD-4 diffractometer equipped with a graphite monochromator (Mo Kα radiation, λ = 0.710 69 Å). Diffraction intensities were collected in the $\omega/2\theta$-scan mode at room temperature. Crystal data and details of measurements are summarized in Table III. The structures were solved by direct methods, which allowed for the location of the Ru atoms, followed by difference Fourier syntheses and subsequent least-squares refinement. Scattering factors for neutral atoms were taken from ref 9. For all calculations the SHELX76 program was used.[9b] An absorption correction was applied for compound **4** by the Walker and Stuart method,[10] once a complete structural model had been obtained and all atoms refined isotropically (correction range 0.88–1.18). All atoms, except the H atoms in **6** and both H atoms and C(ring) atoms in **4**, were treated anisotropically. The H atoms in both species were added in calculated positions (C–H = 1.08 Å), and refined "riding" on their respective C atoms. The H(CH) atoms in **6** were treated with individual isotropic thermal factors, while common isotropic thermal factors were refined for the H(CH) and the H(Me) atoms in **4** and for the H(Me) atoms in **6** [0.11 (2), 0.11 (2), and 0.13 (1) Å^2, respectively]. Fractional atomic coordinates are reported in Tables IV and V, respectively.

Table V. Fractional Atomic Coordinates for 6

atom	x	y	z
Ru(1)	0.31759 (4)	0.66502 (3)	0.23131 (2)
Ru(2)	0.15749 (4)	0.44671 (3)	0.27646 (2)
Ru(3)	0.40620 (4)	0.49196 (3)	0.21382 (2)
Ru(4)	0.08070 (4)	0.61144 (3)	0.29202 (2)
Ru(5)	0.32711 (4)	0.55553 (3)	0.34333 (2)
Ru(6)	0.16446 (4)	0.54963 (3)	0.16036 (2)
C(99)	0.2456 (5)	0.5545 (3)	0.2524 (2)
C(1)	0.3520 (6)	0.7426 (4)	0.2990 (3)
O(1)	0.3656 (5)	0.7918 (3)	0.3373 (3)
C(2)	0.4846 (7)	0.6665 (4)	0.1829 (4)
O(2)	0.5795 (6)	0.6759 (4)	0.1530 (4)
C(3)	0.2340 (7)	0.7415 (4)	0.1752 (3)
O(3)	0.1815 (6)	0.7885 (3)	0.1456 (3)
C(4)	0.1383 (6)	0.3831 (4)	0.3553 (3)
O(4)	0.1197 (6)	0.3438 (3)	0.4020 (2)
C(5)	0.0245 (6)	0.3858 (3)	0.2368 (3)
O(5)	−0.0585 (5)	0.3481 (3)	0.2152 (3)
C(6)	0.3178 (6)	0.3855 (3)	0.2357 (3)
O(6)	0.3465 (5)	0.3192 (3)	0.2281 (3)
C(7)	0.4744 (6)	0.4657 (4)	0.1266 (3)
O(7)	0.5235 (5)	0.4505 (4)	0.0750 (2)
C(8)	−0.0433 (6)	0.5396 (4)	0.3329 (3)
O(8)	−0.1301 (5)	0.5116 (4)	0.3611 (3)
C(9)	−0.0417 (6)	0.6723 (4)	0.2423 (3)
O(9)	−0.1141 (6)	0.7127 (3)	0.2146 (3)
C(10)	0.0794 (7)	0.6863 (4)	0.3635 (3)
O(10)	0.0745 (7)	0.7347 (3)	0.4040 (3)
C(11)	0.5713 (6)	0.4609 (4)	0.2454 (3)
O(11)	0.6754 (5)	0.4412 (4)	0.2617 (3)
C(12)	0.5250 (6)	0.5278 (4)	0.3911 (3)
C(13)	0.4983 (6)	0.6085 (4)	0.4024 (3)
C(14)	0.3752 (6)	0.6296 (4)	0.4336 (3)
C(15)	0.2853 (7)	0.5713 (4)	0.4579 (3)
C(16)	0.3136 (7)	0.4930 (4)	0.4454 (3)
C(17)	0.4326 (7)	0.4689 (4)	0.4106 (3)
C(18)	0.4669 (8)	0.3841 (4)	0.4018 (4)
C(19)	0.6043 (8)	0.6670 (5)	0.3843 (5)
C(20)	0.1631 (8)	0.5912 (6)	0.4999 (4)
C(21)	0.0536 (6)	0.6165 (4)	0.0811 (3)
C(22)	0.1823 (6)	0.6020 (4)	0.0530 (3)
C(23)	0.2285 (6)	0.5231 (4)	0.0510 (3)
C(24)	0.1497 (7)	0.4602 (4)	0.0751 (3)
C(25)	0.0211 (7)	0.4759 (5)	0.0990 (3)
C(26)	−0.0283 (6)	0.5530 (5)	0.1020 (3)
C(27)	0.2677 (8)	0.6651 (4)	0.0216 (3)
C(28)	0.1972 (10)	0.3761 (4)	0.0681 (4)
C(29)	−0.1709 (7)	0.5648 (7)	0.1241 (4)

Crystal Packing Investigation and Methodology. In our approach to crystal packing use is made of the expression PPE = $\sum_i\sum_j[A \exp(-Br_{ij}) - Cr_{ij}^{-6}]$, where PPE represents the packing potential energy[11a] and r_{ij} values represent the nonbonded

(9) (a) International Tables for X-ray Crystallography; Kynoch Press: Birmingham, England, 1975; Vol. IV, pp 99–149. (b) Sheldrick, G. M. SHELX76. *Program for Crystal Structure Determination*; University of Cambridge: Cambridge, England, 1976.

(10) Walker, N.; Stuart, D. *Acta Crystallogr., Sect. B* **1983**, *39*, 158.

atom-atom intermolecular distances. Index i in the summation runs over all atoms of one molecule (chosen as a reference molecule, and index j, over the atoms of the surrounding molecules distributed according to crystal symmetry. A cutoff of 15 Å has been adopted in our calculations. The values of the coefficients A, B, and C used in this work have been taken from the literature[11b] and discussed in previous papers.[12] The results of PPE calculations are used to select the first-neighboring molecules (FNM) among the molecules surrounding the one chosen as reference (RM) on the basis of the contribution to PPE.[12] It should be stressed that this procedure is used only as a convenient means to investigate the molecular environment within the crystalline lattice without pretensions of obtaining "true" (or even approximate) crystal potential energy values.

All calculations were carried out with the aid of the computer program OPEC.[13] SCHAKAL88[14] was used for the graphical representation of the results.

Acknowledgment. We thank the SERC and British Petroleum (P.J.D.) for financial assistance. Financial support by the MURST (Italy) is also acknowledged; D.B., F.G., and B.F.G.J. acknowledge NATO for a travel grant.

Supplementary Material Available: For all species discussed herein, tables of anisotropic thermal parameters, fractional atomic coordinates and thermal parameters, fractional atomic coordinates for the hydrogen atoms, and complete bonds and angles (33 pages). Ordering information is given on any current masthead page.

OM920244V

(11) (a) Kitaigorodsky, A. I. *Molecular Crystal and Molecules*; Academic Press: New York, 1973. (b) Pertsin, A. J.; Kitaigorodsky, A. I. *The Atom-Atom Potential Method*; Springer-Verlag: Berlin, 1987. (c) Gavezzotti, A.; Simonetta, M. *Chem. Rev.* **1981**, *82*, 1. (d) Mirsky, K. *Computing in Crystallography, Proceedings of the International Summer School on Crystallographic Computing*; Delf University Press: Twente, The Netherlands, 1978; p 169.

(12) (a) Braga, D.; Grepioni, F.; Sabatino, P. *J. Chem. Soc., Dalton Trans.* **1990**, 3137. (b) Braga, D.; Grepioni, F. *Organometallics* **1991**, *10*, 1254. (c) Braga, D.; Grepioni, F.; *Organometallics* **1991**, *10*, 2563. (d) Braga, D.; Grepioni, F. *Organometallics* **1992**, *11*, 711.

(13) Gavezzotti, A. OPEC. *Organic Packing Potential Energy Calculations*; University of Milano: Milano, Italy. See also: Gavezzotti, A. *J. Am. Chem. Soc.* **1983**, *195*, 5220.

(14) Keller, E. SCHAKAL88. *Graphical Representation of Molecular Models*; University of Freiburg: Freiburg, FRG.

Alkyne Addition to the Semiinterstitial Boron Atom in Homometallic and Heterometallic Butterfly Clusters: Molecular and Electronic Structures of $HRu_4(CO)_{12}BHC(Ph)CPhH$ and $H(CpW)Ru_3(CO)_{11}BC(Ph)CPhH$

Catherine E. Housecroft,* James S. Humphrey, Ann K. Keep, Dorn M. Matthews, and Nicola J. Seed

University Chemical Laboratory, Lensfield Road, Cambridge CB2 1EW, U.K.

Brian S. Haggerty and Arnold L. Rheingold*

Department of Chemistry, University of Delaware, Newark, Delaware 19716

Received July 13, 1992

The clusters $HRu_4(CO)_{12}BH_2$ and $H(CpW)Ru_3(CO)_{11}BH$ both undergo alkyne coupling reactions with diphenylacetylene to form $HRu_4(CO)_{12}BHC(Ph)CPhH$, **1**, and $H(CpW)Ru_3(CO)_{11}BC(Ph)CPhH$, **2**, respectively. In each case one Ru-H-B bridging hydrogen atom is transferred to the alkyne and a B-C bond is formed. The molecular structures of the two products have been determined by single-crystal X-ray diffraction, and a comparison of the two structures shows that the introduction of the heterometal atom into the butterfly framework of the precursor has a significant influence upon the nature of the product obtained. **1**: monoclinic, $P2_1/c$; a = 9.758 (2), b = 36.653 (8), c = 17.131 (4) Å; β = 101.92 (2)°; V = 5996 (3) Å^3; Z = 8; $R(F)$ = 5.56%. **2**: monoclinic, $P2_1/n$; a = 14.324 (4), b = 13.983 (3), c = 16.618 (3) Å; β = 108.47 (2)°; V = 3157 (2) Å^3; Z = 4; $R(F)$ = 4.35%. The four ruthenium atoms in **1** define a spiked triangle; the boron atom interacts with all four metal atoms, and the alkyne resides in a position such that it bonds to the boron atom and two ruthenium atoms including that of the spike. In contrast, the tungsten and three ruthenium atoms in **2** retain the butterfly skeleton of the precursor and the alkyne interacts with the boron atom and one ruthenium atom only. Differences in bonding with respect to boron-alkyne coupling in **1** and **2** are addressed by use of the Fenske-Hall molecular orbital method, and appropriate electron counting schemes for the two compounds are assessed in the light of the results of the MO calculations.

In a preliminary publication[1] we reported that the reaction of diphenylacetylene with the tetraruthenaborane $HRu_4(CO)_{12}BH_2$ resulted in insertion of the alkyne into the butterfly framework of $HRu_4(CO)_{12}BH_2$ with concomitant B-C bond formation, B-H bond activation, and Ru_4-skeletal opening (Figure 1a). This result was in contrast to that observed for the reaction of PhC≡CPh with $H_2Ru_4(CO)_{12}C$ (which exists as the mixture of isomers $H_2Ru_4(CO)_{12}C$ and $HRu_4(CO)_{12}CH$)[2] or $[Ru_4(CO)_{12}N]^-$[3]

(1) Chipperfield, A. K.; Haggerty, B. S.; Housecroft, C. E.; Rheingold, A. L. *J. Chem. Soc., Chem. Commun.* **1990**, 1174.

(2) Dutton, T.; Johnson, B. F. G.; Lewis, J.; Owen, S. M.; Raithby, P. R. *J. Chem. Soc., Chem. Commun.* **1988**, 1423.

(3) Blohm, M.; Gladfelter, W. L. *Organometallics* **1986**, *5*, 1049.

0276-7333/92/2311-4048$03.00/0